

Transport through normal metal-graphene contacts

Y. M. Blanter

Kavli Institute of Nanoscience, Delft University of Technology, Lorentzweg 1, 2628 CJC Delft, The Netherlands

Ivar Martin

Theoretical Division, Los Alamos National Laboratory, Los Alamos, New Mexico, 87544, USA

(Dated: February 8, 2020)

Conductance of zigzag interfaces between graphene sheet and normal metal is investigated in the tight-binding approximation. Boundary conditions, valid for a variety of scattering problems, are constructed and applied to the normal metal-graphene-normal metal (NGN) junctions. At the Dirac point, the conductance is determined solely by the evanescent modes and is inversely proportional to the length of the junction. Away from the Dirac point, the propagating modes' contribution dominates. We also observe that even in the junctions with high interface resistance, for certain modes, ideal transmission is possible via Fabry-Perot like resonances.

Recent experimental studies [1, 2, 3, 4] uncovered unusual properties of graphene (graphite monolayers and bilayers), strongly contrasting with the common knowledge inherited from studies of metals. This difference originates from the fact that electrons in graphene monolayers obey the Dirac (rather than the Schrödinger) equation. Thus, one has an opportunity to study properties of the Dirac fermions in a table-top experiment. Predictions of relativistic effects including the Klein tunneling [5] and Zitterbewegung [6] have been made. "Ordinary" phenomena, e.g., weak localization [7] or Andreev reflection [8], are also strongly modified in graphene as compared to normal metals.

The most easily accessible measurements in graphene are those of electrical transport. Theoretically, one way of understanding them is to extend the Landauer theory to graphene sheets, considering them as a junction between two reservoirs. So far, a common point was to describe reservoirs as bulk disordered graphene [8, 9, 10]. This approach considerably facilitates calculations; however, its relation to the experimental situation, with contacts made of normal metals, requires additional clarification. A first step in this direction was recently made by Schomerus [11] who compared resistances of NGN contacts with a zigzag interface, and graphene-graphene (GGG) contacts. He considered the special case of equal overlap integrals between all neighboring sites in the tight-binding model. He found that if the graphene sheet is biased to the Dirac point, so that there are no propagating modes through graphene, the difference between NGN and GGG junctions is only quantitative. Outside this regime, the behavior of the contacts may strongly depend on the type of the leads and the interface. In this Letter, we study this dependence for the simplest case of square-lattice leads and zigzag interfaces, and find a number of fundamental results.

Below, we consider within the tight-binding approximation the general problem of transmission through the NG interfaces and NGN structures for arbitrary overlap integrals t_s , t_g , and t^0 , in square-lattice normal metals,

graphene, and at the interface, respectively. From the lattice Schrödinger equation, we derive the wave-function matching conditions at the interfaces. We apply them first to the scattering off the NG interface and determine the reflection probability back to the normal metal. Then, we turn to the conductance of an NGN junction. It is the sum of two contributions coming from propagating and evanescent modes in graphene. The number of the available propagating modes is proportional to the radius of the Dirac cone q_g taken at the gate voltage energy eV_g , $q_g \propto V_g$. Their contribution to conductivity is therefore proportional to V_g ; it is independent of the graphene length L in the limiting cases $q_g L \ll 1$ and $q_g L \gg 1$. At the Dirac point ($V_g = 0$), there are no propagating modes; however, there is a contribution to conductivity from the evanescent modes that obeys the Ohm's law, i.e. is inversely proportional to the length of the graphene strip L [10, 11]. For non-zero gate voltage V_g the contribution of evanescent modes crosses over to $L^{-1}(q_g L)^3$ behavior for $q_g L \gg 1$. We also observe that for the symmetric case $t^0 = t_s t_g$, a narrow graphene strip is ideally transmitting, both through the propagating and evanescent states. However, even for opaque interfaces, $t^0 \neq t_s t_g$, we find that some modes transmit ideally, in a direct analogy to the Fabry-Perot resonances in a double-barrier structure.

NG interface. We consider an interface between normal metal with the square lattice and graphene with the periods a_s and $a_g = a_s = \frac{1}{\sqrt{3}}$, respectively, Fig. 1. We assume that the normal metal is taken around the half-filling, so that the Fermi surface is nearly a square, whereas the graphene is tuned close to the Dirac point. In the normal metal, the wave function is a plane wave, $c(r) = e^{ik_s x} + r e^{-ik_s x} e^{ik_g y}$; $x < 0$, defined on the sites of the square lattice. First and second terms describe incident and reflected waves, respectively. In graphene, one has to define two transmitted waves corresponding to two sublattices a and b , $d^a(r); d^b(r)$.

For the zigzag interface, the wave vector component along the interface k_y is conserved, and thus the two-

dimensional scattering problem reduces to a collection of one-dimensional problems for different values of k_y . The transverse component of wavevector (k_x) is not conserved and must be found from the energy conservation.

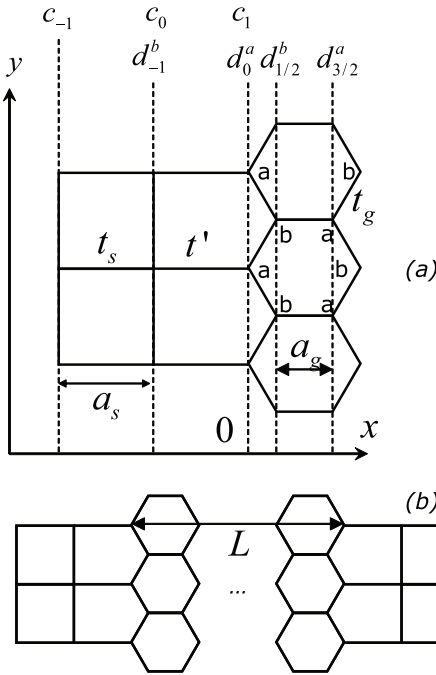


FIG. 1: (a) A zigzag interface between a square and graphene lattices. Sites belonging to the two sublattices in graphene are shown by letters a and b. On the top, boundary conditions are sketched: We introduced two columns of continuous amplitudes, c_1 in graphene, and d_{-1}^b in the square lattice, used for wave functions matching at the interface. (b) A NGN contact.

In the tight-binding model, the amplitudes obey the lattice Schrodinger equations. In particular, at the interface, we obtain the following set of equations,

$$\begin{aligned} E c_0 &= 2t_s c_0 \cos k_y a_s - t_g c_1 - t_g d_0^b; \\ E d_0^b &= t_g c_0 - 2t_g \cos \frac{3k_y a_g}{2} d_{1/2}^b; \\ E d_{1/2}^b &= t_g d_{3/2}^b - 2t_g \cos \frac{3k_y a_g}{2} d_0^b; \end{aligned} \quad (1)$$

where we moved to discrete notations, explained in Fig. 1: The subscript shows the distance from the interface, measured in corresponding lattice constants.

Away from the interface, the solution of the Schrodinger equation is a superposition of plane (or evanescent, see below) waves, with the energies

$$\begin{aligned} E_s &= 2t_s (\cos k_s a_s + \cos k_y a_s); \\ E_g &= t_g \frac{1 + 4 \cos \frac{3k_y a_g}{2}}{2} \cos \frac{3k_y a_g}{2} + \cos \frac{3k_g a_g}{2} \end{aligned}$$

In this Letter, we are mainly interested in the low-energy regime, $E \ll t_g$. In this regime, the energy can be

expanded in the vicinity of the points where it turns to zero (K points), $k_g = q_x$, $k_y = \frac{4}{3} = (3a_g) + q_y$, $E = (3t_g/2)q$, with $q = (q_x^2 + q_y^2)^{1/2}$. For concreteness, we only consider the "upper" Dirac point, $k_y = \frac{4}{3} = (3a_g)$; by symmetry, the "lower" one contributes to transport identically. For propagating waves, from the graphene (lattice) Schrodinger equation we obtain $d^b = ie^{i' d^a}$, where $\tan' = q_y/q_x$.

The interface equations, Eqs. (1) can be equivalently recast in the form of the wave function matching, which is convenient when considering more complex scattering, such as NGN (see below). This can be done by continuing the wave functions across the interface. Introducing continuous wave function elements c_1 and d_{-1}^b , the first two equations of Eqs. (1) become

$$t_s^0 d_0^a = t_s c_1; \quad t_g d_{-1}^b = t_g^0 c_0;$$

These are general boundary conditions and can be applied to a scattering problem with arbitrary arrangements. For example, scattering from N to G can be obtained if we set

$$c_0 = 1 + r; \quad c_1 = e^{ik_s a_s} + r e^{-ik_s a_s}; \quad d_{-1}^b = d_0^b e^{-ik_g a_g};$$

Substituting into the above boundary conditions, we find the equations connecting the amplitudes of the waves,

$$t_s (e^{ik_s a_s} + r e^{-ik_s a_s}) = t_s^0 d_0^a; \quad (3)$$

$$t_g^0 (1 + r) = t_g d_0^b e^{-ik_g a_g}; \quad (4)$$

Thus, for the reflection coefficient $R = |r|^2$, at low energies ($k_g a_g \ll 1$), we find

$$R = \frac{1 + 2 \sin(\theta + k_s a_s)}{1 + 2 \sin(\theta - k_s a_s)}; \quad \frac{t_g^0}{t_s t_g}; \quad (5)$$

Near half-filling, $k_s a_s = \pi/3$; however, these results apply to the case of arbitrary filling, where $k_s a_s \neq \pi/3$. As anticipated, for an opaque interface $t_g^0 = t_s t_g$, the reflection approaches 1. Note also that one can only match the wave vectors in the x-direction for a very limited set of wave vectors around $k_s a_s = \pi/3$; all other states are ideally reflected by the interface.

NGN interface: propagating modes. Consider now a graphene sheet of length L connected to two square-metal electrodes (with the same overlap integral) by two ideal zigzag interfaces. Note that such an arrangement is only possible provided $L = a_g (3N + 1)/2$ with an odd-integer N . We take the wave function in the left electrode in the same form as before, $c(r) = e^{ik_s x} + r e^{-ik_s x} e^{ik_y y}$, (2) the wave function in graphene as a combination of left- and right-moving waves for each sublattice, and the wave function in the right electrode as the transmitted wave $f(r) = w \exp(ik_s x + ik_y y)$.

The equations for the NGN structure read

$$t_s^0 c_0 = t_g (d_{-1}^b + d_r^b); \quad (6)$$

$$t_s c_1 = t^0 (d_1^a + d_r^a)_0; \quad (7)$$

$$t^0 f_0 = t_g (d_1^a + d_r^a)_{(3N+1)=2}; \quad (8)$$

$$t_s f_1 = t^0 (d_1^b + d_r^b)_{(3N+3)=2}; \quad (9)$$

In addition to c_1 and d_{-1}^b , we introduced two more "unphysical" amplitudes, $d_{(3N+3)=2}^a$ and f_1 . We use now $d_r^b = ie' d_r^a$ and $d_1^b = ie' d_1^a$, where ' in both expressions is defined for the right-moving electrons. Solving this scattering problem for $qa_g = 1$, we find for the transmission amplitude

$$w = 2i \cos' \sin k_s a_s e^{ik_s a_s} J^{-1}; \quad (10)$$

$$J = e^{ik_s a_s} \cos' (qL \cos') - 2 \sin (qL \cos') e^{ik_s a_s} \cos' (qL \cos');$$

Note that for $qL = 1$ and $t^0 = t_s t_g$, the junction is ideally transmitting.

Evanescent modes. For a finite length of the graphene strip, there are also solutions which are not propagating, but rather exponentially increasing or decreasing as $e^{-k_s x}$ (the evanescent states. Their energy reads

$$E = \frac{3t_g}{2} \frac{q}{q_y^2 - k_s^2};$$

which is defined as far as $j_x j_y j_z$. Similar to the propagating case, we can find the relation between the components of the graphene wavefunction,

$$d^b = \frac{q_y + j_x}{q_y - j_x} d^a; \quad (11)$$

where corresponds to E . In the following, we consider the positive energy branch, E_+ . While there is no propagation in the evanescent case, we can still define the right ($x > 0$) and left ($x < 0$) components of the wave function (the wave "propagates" in the direction of decay. For these components, $d_r^b = Z d_r^a$; $d_1^b = Z^{-1} d_1^a$, where $Z = (q_y + j_x)/(q_y - j_x) = (q_y - j_x j_z)$. The transmission amplitude through the evanescent modes becomes

$$w = 2i \sinh \sin k_s a_s e^{ik_s a_s} J^{-1}; \quad (12)$$

$$J = e^{ik_s a_s} \sinh (xL + \dots) - 2 \sinh xL + e^{ik_s a_s} \sinh (xL - \dots);$$

with $= \ln Z$. Clearly, for $t_g t_s = t^0$ and $xL = 1$ we obtain again the perfect transmission.

Current and conductance. The current through the junction is expressed as

$$I_x = eW \frac{dk_s dk_y}{(2\pi)^2} v_x jw (k_s; k_y) j^2 \\ = \frac{eW}{(2\pi)^2 h} \frac{Z}{eV_g + ev} \frac{Z}{Z} dE dk_y jw (k_s; k_y) j^2; \quad (13)$$

where W is the width of the graphene strip in the y -direction, and $v_x = h^2 e E_s / \Omega k_s$ is the group velocity. Let us first consider the contribution of propagating states. The integration is carried over the momenta

for which $v_x > 0$. In the linear regime, we obtain the conductance

$$\frac{G_{tr}}{G_Q} = \frac{eW q_g}{G_Q} \frac{Z}{jw j^2 \cos' d'}; \quad (14)$$

with $q_g = 2eV_g j/(3t_g a_g)$ and $G_Q = e^2/2h$ being the conductance quantum.

For short junctions, $q_g L \ll 1$, the transmission coefficient does not depend on the angle, and we obtain

$$\frac{G_{tr}}{G_Q} = \frac{2W q_g}{G_Q} \frac{4 \sin^2 k_s a_s}{1 + 2 \cos k_s a_s}; \quad (15)$$

The quantity $2W q_g$ can be interpreted as a "number of transport channels." In the ideal case, $= 1$, the conductance equals $2W q_g G_Q = 1$.

For longer junctions, $q_g L \gg 1$, we use the fact that $\cos(q_g L \cos')$ is a rapidly oscillating function of the angle'. In particular, for $= 1$, we have

$$jw j^2 = \cos^2' \sin^2 k_s a_s \sin^2 k_s a_s \cos^2' \cos^2 (q_g L \cos') \\ + (1 - \cos k_s a_s \sin')^2 \sin^2 (q_g L \cos')^{-1}; \quad (16)$$

Between the points ' n and ' $n+1$, with $\cos' n = n/(q_g L)$, the integral in Eq. (13) can be calculated assuming that the slow functions \cos' and \sin' are constant and equal to $\cos' n$ and $\sin' n$ everywhere except for in combination $\cos(q_g L \cos')$. Then Eq. (13) becomes a sum over the periods n of $\cos(q_g L \cos')$. Converting the sum into an integral, one obtains

$$\frac{G_{tr}}{G_Q} = \frac{W q_g (1 - \sin k_s a_s)}{4 \sin k_s a_s \cos^2 k_s a_s}; \quad (17)$$

This result is length independent, similar to Eq. (14), but for $k_s a_s = -3$ the conductance of a long graphene layer is suppressed as compared to a short layer.

For untransparent interfaces, $= 1$, the transmission coefficient can be approximated as

$$jw j^2 = \frac{4 \sin^2 k_s a_s \cos^2'}{\cos^2 (q_g L \cos') j^2 + 4 \sin^2 k_s a_s \sin^2 (q_g L \cos') j^2}; \quad (18)$$

This expression has the structure similar to that of resonant tunneling for a double barrier: Typically the numerator is of order of $j^2 \ll 1$, whereas the denominator is of order 1, and the transmission probability is small. However, for certain directions ' m of the wave vector, when the cosine of the denominator vanishes, the transmission becomes ideal. One can expand the expression around the resonance ' m to obtain Breit-Wigner structure of the resonance, ' $= ' m + ' , ' , ' - 1$,

$$jw j^2 = \frac{4 \sin^2 k_s a_s \cos^2 '}{(q_g L \sin ' m)^2 j^2 + 4 \sin^2 k_s a_s \cos^2 ' m}; \quad (19)$$

Typically one can omit 1 as compared to $q_g L \sin' m$ in the denominator. The main contribution to the current comes from the directions around the resonances. Integrating the Bethe-Wigner expressions and transforming the resulting sum over m into an integral, we obtain

$$G_{tr} = G_Q = W q_g \sin k_s a_s : \quad (20)$$

Note, that here the conductance of a long layer is proportional to W and thus parametrically exceeds the conductance of a short layer (proportional to W^2). This effect is due to the resonant structure of Eq. (18).

Let us turn now to the contribution of the evanescent modes. In the vicinity of the Dirac point, the number of propagating states vanishes as E , and thus the contribution of the large number of evanescent states with $j_x j_y$ becomes dominant. At zero energy, $E = 0$, and $q_y > 0$, one has $Z = 1$. Thus

$$W = \frac{2i \sin k_s a_s e^{ik_s a_s}}{1 - e^{-ik_s a_s} e^{-x/L} + e^{ik_s a_s} e^{-x/L}} : \quad (21)$$

For the ideal case, $Z = 1$, we find

$$j_y j_x^2 = \frac{2 \sin^2 k_s a_s}{\cosh 2x/L + \cos 2k_s a_s} ; \quad (22)$$

and thus the conductance

$$\frac{G_{ev}}{G_Q} = \frac{W}{L} \int_1^{Z+1} \frac{dx}{\cosh x + \cos 2k_s a_s} \quad (23)$$

$$= \frac{2W}{L} k_s a_s \tan k_s a_s \quad (24)$$

in agreement with the result by Schomerus [11].

For $Z = 1$, one has $j_y j_x^2 = 4 \sin^2 k_s a_s e^{-2x/L}$, and thus conductance becomes

$$\frac{G_{ev}}{G_Q} = \frac{4^2 W}{L} \int_1^{Z+1} \frac{dk_y}{\cosh x + \cos 2j_x j_y} e^{-2j_x j_y L} \\ = \frac{2W}{L} \sin^2 k_s a_s : \quad (25)$$

Away from zero energy, $qL \neq 1$, the contribution of evanescent modes rapidly vanishes. Indeed, by noting that conductivity is contributed by the states with $j_x j_y \neq 0$, and thus $dk_y / (x=q) dx$, we find

$$\frac{G_{ev}}{G_Q} = \frac{12}{L} \frac{(3)W}{(q_g L)^3} \int_1^{\infty} \frac{\sin^2 k_s a_s}{e^{-ik_s a_s} + e^{ik_s a_s} - 2j_x^2} : \quad (26)$$

Here, (3) is the Zeta function, with $(3) = 1.2021$. This result disagrees with Ref. [11], which finds $G_{ev} / G_Q \approx 1$ for all gate voltages; we currently do not understand the reasons of this discrepancy.

In conclusion, we constructed the wave-function matching conditions at the zigzag interfaces between square (N) and graphene (G) lattices, and determined transport properties of the NGN structure, concentrating

on the regimes of ideal interface ($t_g^2 = t_a t_s$) and highly resistive interface ($t_g^2 \ll t_a t_s$). In accordance with earlier predictions, at the Dirac point the conductance is dominated by the evanescent modes and scales inversely proportional to the length of the contact L . However, the situation changes qualitatively as soon as one departs from the Dirac point (for instance, by changing the electron concentration via the gate voltage V_G). The propagating modes start to contribute to the conductance. For small V_G , such that $q_g L \ll 1$, their contribution is length-independent; in particular we find that for ideal interfaces the transmission equals one independently of the angle of incidence. Further yet from the Dirac point, $q_g L \gg 1$, the conductance is determined by the propagating modes, whereas the evanescent modes' contribution decays as L^{-4} .

Besides looking at the low transport bias regime considered above, it also may be interesting to study the non-linear $I-V_t$ characteristics. Our results suggest that with increasing transport voltage V_t , the contribution of the evanescent modes to the current saturates with voltage beyond $V_t > t_g a_g = L$, while the propagating modes' contribution increases as V_t^2 .

The zigzag interface considered in this Letter is the simplest case of a contact: The periods of the lattices match, $a_s = \sqrt{3} a_g$, and the momentum component k_y along the interface is conserved. In real experimental situations both of these conditions will be difficult to realize: The interfaces are disordered, and the lattice periods may be incommensurate. This Letter illustrates an importance of the interface contribution to the transport and provides the basis for future research in this direction.

We thank S. Trugman for useful discussions. The authors acknowledge Aspen Center for Physics, where this research was initiated. This work was supported in part by US DOE.

- [1] K. S. Novoselov et al., *Science* **306**, 666 (2004).
- [2] Y. Zhang et al., *Nature* **438**, 201 (2005).
- [3] E. R. Rollings et al., cond-mat/0512226; X. Wu et al., cond-mat/0611339.
- [4] H. B. Heersche et al., cond-mat/0612121.
- [5] V. V. Cheianov and V. I. Fal'ko, *Phys. Rev. B* **74**, 041403 (2006); M. I. Katsnelson, K. S. Novoselov, and A. K. Geim, *Nature Phys.* **2**, 620 (2006).
- [6] M. I. Katsnelson, *Eur. Phys. J. B* **51**, 157 (2006); B. Trauzettel, Ya. M. Blanter, and A. F. Morpurgo, cond-mat/0606505.
- [7] E. M. McCann et al., *Phys. Rev. Lett.* **97**, 146805 (2006).
- [8] C. W. J. Beenakker, *Phys. Rev. Lett.* **97**, 067007 (2006).
- [9] N. M. R. Peres, A. H. Castro Neto, and F. Guinea, *Phys. Rev. B* **73**, 195411 (2006).
- [10] J. Tworzydlo et al., *Phys. Rev. Lett.* **96**, 246802 (2006).
- [11] H. Schomerus, cond-mat/0611209.